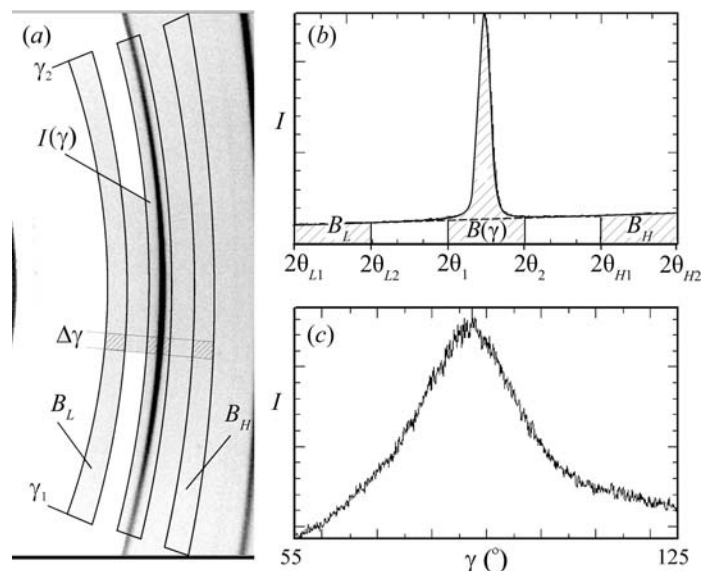


## 2.5. TWO-DIMENSIONAL POWDER DIFFRACTION

**Figure 2.5.21**

Pole-figure data processing: (a) a frame with the  $2\theta$  integration ranges for the (220) ring; (b)  $2\theta$  profile showing the background and peak; (c) integrated intensity distribution as a function of  $\gamma$ .

expressed as

$$I(\gamma) = \int_{2\theta_1}^{2\theta_2} J(2\theta, \gamma) d(2\theta), \quad \gamma_1 \leq \gamma \leq \gamma_2. \quad (2.5.61)$$

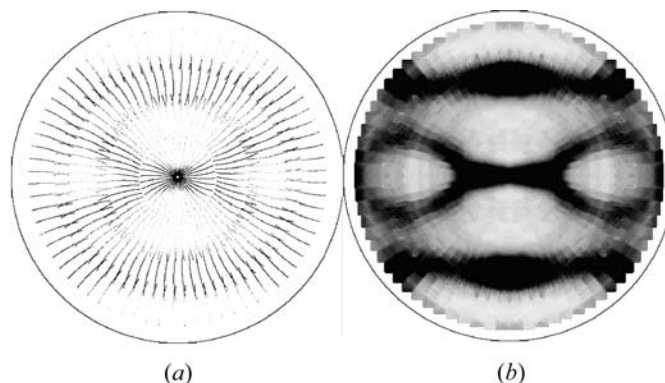
A similar equation can be used for  $2\theta$  integration of the low and high backgrounds  $B_L(\gamma)$  and  $B_H(\gamma)$ . Assuming a linear background change in the vicinity of the  $2\theta$  peak, the background under the peak,  $B(\gamma)$ , is then given by

$$B(\gamma) = B_L(\gamma) \frac{(2\theta_2 - 2\theta_1)(2\theta_{H2} + 2\theta_{H1} - 2\theta_2 - 2\theta_1)}{(2\theta_{L2} - 2\theta_{L1})(2\theta_{H2} + 2\theta_{H1} - 2\theta_{L2} - 2\theta_{L1})} + B_H(\gamma) \frac{(2\theta_2 - 2\theta_1)(2\theta_2 + 2\theta_1 - 2\theta_{L2} - 2\theta_{L1})}{(2\theta_{H2} - 2\theta_{H1})(2\theta_{H2} + 2\theta_{H1} - 2\theta_{L2} - 2\theta_{L1})}. \quad (2.5.62)$$

Then the background  $B(\gamma)$  can be subtracted from the integrated intensity distribution  $I(\gamma)$ .

The algorithms of  $\gamma$  integration given in Section 2.5.4.2.3 can be easily modified for  $2\theta$  integration by exchanging  $\gamma$  and  $2\theta$  in the equations. Algorithms with solid-angle normalization should be used to get consistent integrated intensity over all areas of the detector. The  $2\theta$ -integrated intensity distribution can then be mapped onto a pole figure based on the fundamental equations (2.5.53) and (2.5.54). When a pole-figure pixel is overlapped by more than one data point from different scans, as shown in the region covered by two scans in Fig. 2.5.20(b), the average value should be mapped to that pole-figure pixel. Fig. 2.5.22(a) shows pole-density mappings on the pole figure. There are big gaps between the measured pole-density data points due to the large  $\varphi$ -scan steps of  $5^\circ$ .

All factors affecting relative intensities, such as Lorentz, polarization, air scattering, and Be-window and sample absorption, will have an effect on the measured pole densities for the pole figures. Some or all these corrections may be applied to the diffraction frames before  $2\theta$  integration if the texture study demands high accuracy in the relative pole densities. Among these factors, the most important factor is sample absorption, since data sets for pole figures are typically collected at several different incident angles. A ridge between the pole-density

**Figure 2.5.22**

Pole-figure processing: (a)  $I(\gamma)$  mapped to the pole figure; (b) Pole figure after interpolation and symmetry processing.

regions covered by two different incident angles may be observed if sample absorption is not properly corrected.

## 2.5.4.2.5. Pole-figure interpolation and use of symmetry

The pole figure is stored and displayed as a bitmap image. The pole-density data from the data set may not fill up all the pixels of the pole-figure image. In order to generate a smooth pole figure, the unmapped pixels are filled with values generated from the interpolation of the surrounding pixels. A linear interpolation within a defined box is sufficient to fill the unmapped pixels. The size of the box should be properly chosen. A box that is too small may not be able to fill all unmapped pixels and a box that is too big may have a smearing effect on the pole figure, especially if a sharp pole figure is processed. All the gaps between the measured pole-density points are filled after this interpolation. For a sample with sharp texture, smaller  $\varphi$ -scan steps should be used.

All pole figures possess symmetry as a consequence of the Laue symmetry of the crystallites in the sample. This symmetry can be used to fill in values for pixels in the pole figure for which data were not measured, or to smooth the pole figure. For example, orthorhombic materials exhibit  $mmm$  symmetry, thus one needs to collect only an octant or quadrant of the pole sphere to generate the entire pole figure. The pole figures of materials with higher symmetry may be treated by using lower symmetry in the processing. For instance, one can use  $2/m$  or  $mmm$  symmetry for hexagonal materials and  $mmm$  for cubic materials. In symmetry processing, all the symmetry-equivalent pole-figure pixels are filled by the average value of the measured pixels. For the unmeasured pole-figure pixels, this symmetry processing fills in a value from the average of all the equivalent pixels. For the measured pixels, this average processing serves as a smoothing function. Fig. 2.5.22(b) shows the results after both interpolation and use of symmetry.

## 2.5.4.2.6. Orientation relationship

A 2D-XRD system can measure texture from a sample containing a single phase, multiple phases or single crystals. The orientation relationship between different phases, or thin films and substrates, can be revealed because data are collected from all phases of the sample simultaneously. One example is the measurement of pole figures for a magnetron sputter-deposited Cu film on an Si wafer (He *et al.*, 2005). Fig. 2.5.23 shows the overlapped pole figures of the Cu (111) film and Si (400) substrate in a 2D pole figure (a) and 3D surface plot (b). The three sharp spots from the (400) spots of the Si wafer show the wafer cut orientation of (111). The Cu (111) pole density maxi-